Communication

Evaluation of the Binding Kinetics of RHEB with mTORC1 by In-cell and In vitro Assays

Raef Shams [1,2], Yoshihiro Ito [1,3] and Hideyuki Miyatake [2,3,*]

[1] Emergent Bioengineering Materials Research Team, RIKEN Center for Emergent Matter Science, RIKEN, Wako, Saitama 351-0198, Japan; raef.shams@riken.jp (R. S.); y-ito@riken.jp (Y. I)
[2] Department of Life Science, Graduate School of Science and Engineering, Saitama University, Saitama city, Saitama 338-8570, Japan; miyatake@riken.jp (H. M.)
[3] Nano Medical Engineering Laboratory, RIKEN Cluster for Pioneering Research, RIKEN, Wako, Saitama 351-0198, Japan
* Correspondence: miyatake@riken.jp; Tel.: + 81-48-467-4979

Abstract: The mammalian/mechanistic target of rapamycin complex 1 (mTORC1) is activated by the small G-protein, RHEB-GTPase. On lysosome, RHEB activates mTORC1 by binding the domains of N-heat, M-heat, and FAT, which allosterically regulates ATP binding in the active site for further phosphorylation. The crucial role of RHEB in regulating growth and survival through mTORC1, makes it a targetable site for anti-cancer therapeutics. However, the binding kinetics of RHEB to mTORC1 is still unknown at the molecular level. Therefore, we studied the kinetics by in vitro and in-cell protein-protein interaction (PPI) assays. For this, we used the split-luciferase system (Nano-BiT®) for in-cell studies, and prepared proteins for the in vitro measurements. Consequently, it was shown that RHEB binds to the whole mTOR both in the presence or absence of GTPγS, with five-fold weaker affinity in the presence of GTPγS. Also, RHEB bound to the truncated mTOR fragments of N-heat domain (60-167) and M-heat domain (967-1023) in a GTP independent manner. Furthermore, RHEB bound to the truncated kinase domain (2148-2300) with higher affinity also in GTP independently. In conclusion, RHEB binds two different binding sites of mTOR, which probably regulates the kinase activity of mTOR through multiple different molecular mechanisms.

Keywords: mTORC1; RHEB; G-Protein; Allosteric activation; Kinase domain; Binding kinetics.

1. Introduction

The mammalian/mechanistic target of rapamycin (mTOR) regulates cell growth and survival through the modulation of the metabolic pathways [1,2]. mTOR assembles in two different complexes, mTOR complex 1 (mTORC1) and mTOR complex 2 (mTORC2), which are involved in different upstream or downstream signals[1,3]. In the mTORC1, mTOR is a kinase complexed with other proteins, Raptor, mLST8, Deptor and PRAS40, to regulate the recruiting and phosphorylation of substrates (Figure 1a) [3,4]. In response to growth factors and nutrients, mTORC1 regulates a variety of life phenomenon; synthesis of proteins, lipids and nucleotides, cell proliferation and autophagy [1]. Recently, several studies have revealed the molecular mechanisms of mTORC1 kinase activation by amino acids and growth factors [5-7].

Early biochemical studies suggested that the small G-protein, Ras homolog enriched in brain (RHEB) was involved in the activation of mTORC1 [8-10]. In addition, it was found that the tuberous sclerosis complex 1/2 (TSC1/2), the upstream negative regulators of mTORC1, served as a GTPase-activating protein for RHEB [7,11,12]. Through this, the active RHEB-GTPase positively modulates the mTORC1 activity. Later, it was shown that RHEB bound to the ATP binding domain (2148-2300) in GTP-independent manner [10], which did not activate the kinase activity. Therefore, the functional aspect of the binding has remained to be addressed [10].

Preprints (www.preprints.org) | NOT PEER-REVIEWED | Posted: 11 June 2021 doi:10.20944/preprints202106.0309.v1

While it was reported that RHEB activated mTORC1 by antagonizing a negative regulator FKBP38, a member of FK506-binding protein family, in a GTP-dependent manner [8]. On the other hand, growth factors and nutrients promote the binding of RHEB to mTOR, whereby promoting the kinase activity of mTORC1 [8]. Recently, the cryo-EM structure of mTORC1/RHEB-GTPγS complex showed a scenario how mTORC1 was activated by RHEB-GTP [4]. In the complex, RHEB-GTPγS bound to a binding site constituted by the N-heat, FAT, and M-heat domains far from the ATP binding site. It caused a large conformational change of mTOR, which in turn allosterically rearranged the ATP binding site to turn-on the kinase activity [4]. Since RHEB is farnesylated into the lysosome membrane [12], the mTORC1 activation process occurs onto the lysosome surface in response to growth factors and nutrients through two parallel and integrated pathways (Figure S1). At first, the RHEB-GTPase is being activated through the growth factors / TSC pathway which enables RHEB to be charged by GTP [7,12]. Then, the mTORC1 was translocated onto the lysosome surface in response to the increasing concentration of amino acids [5,6]. The Raptor subunit of mTORC1 was anchored by the Rag GTPase-Ragulator complex onto the lysosome surface, offering the binding scaffold for RHEB-GTP [13,14]. On the lysosome surface, two RHEB-GTP cooperatively activated mTORC1 to phosphorylate 4E-BP1 [4]. The stoichiometry obtained, however, did not involve the binding kinetics of the RHEB to mTOR protein-protein interaction (PPI). Therefore, we aimed in this study to reveal the kinetics of the RHEB to mTOR by using the in-cell and in vitro PPI methods [15].

2. Results and Discussion

At first, we studied the in vitro binding kinetics of RHEB to the whole mTOR. Briefly, the Halo-tagged full-length mTOR (aa 1-2,549; Kazusa-Promega) was overexpressed by pFN21A/ HEK239 cell system, and purified by the HaloLink™ resin (Promega, USA) (Figure S2 and Figure 1b). The artificial gene of RHEB was synthesized (Eurofins Genomics) and subcloned into pET15b expression vector (Novagen). 6xHis-tagged RHEB (aa 1-169) was overexpressed by BL21(DE3) E. coli system (Nippon gene) and purified by Ni-NTA and Superdex-200 columns (GE Healthcare, USA) (Figure S3 and Figure 1c). Then, we established the in vitro method for PPI by the AlphaLISA system including the anti-IgG donor beads and anti-6xHis acceptor beads (PerkinElmer, USA; Figure 1d and Figure S4).

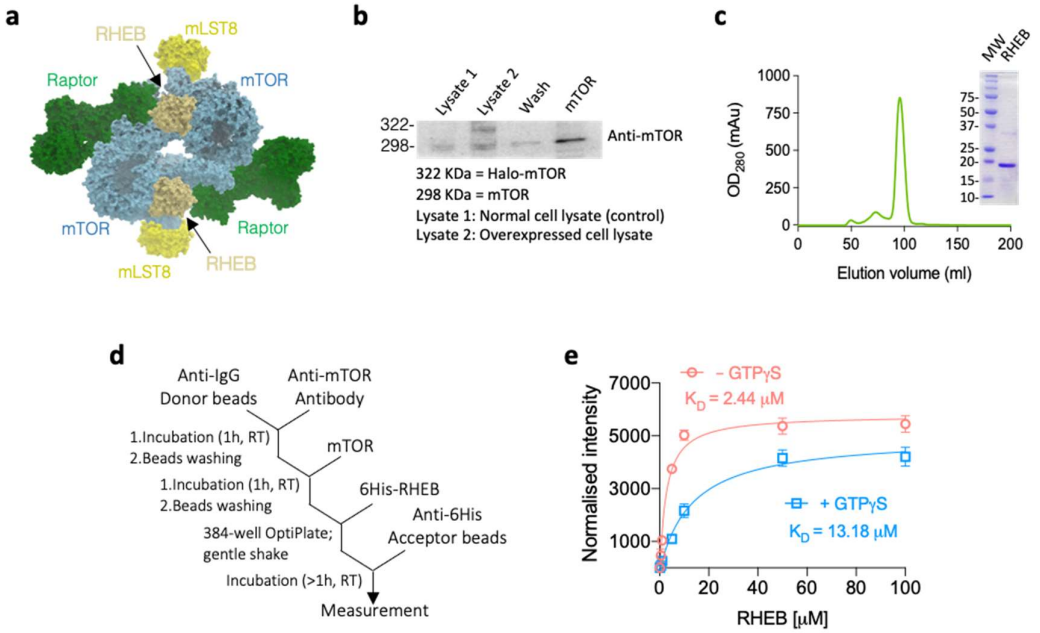

Figure 1. Binding kinetics of RHEB-mTOR. (**a**) Molecular structure of homodimer mTORC1 showing the complex components except Deptor or PRAS40 (PDB ID: 6BCU) solved by the cryo-EM. (**b**) Western blot analysis of the different stages of mTOR purification showing the overexpression of the Halo-tagged mTOR. (**c**) Gel-filtration profile and the corresponding Coomassie blue-stained SDS-PAGE of the purified 6xHis-RHEB (MW: Molecular Weight; KDa). (**d**) Protocol of AlphaLISA® assay to measure the binding affinity of RHEB for mTOR. A variety concentration of 6xHis-RHEB and excess amount of anti-6His acceptor beads were used (See Figure S2 for details). (**e**) Binding of RHEB to mTOR in the presence (blue plot) or absence (red plot) of GTPγS. Data shown as mean of two independent experiments (n=3 replicates each) ± standard deviation. The signal was normalized to the background. The equilibrium dissociation constants (K_D) are shown.

Preprints (www.preprints.org) | NOT PEER-REVIEWED | Posted: 11 June 2021 doi:10.20944/preprints202106.0309.v1

As a result, we observed that RHEB bound to mTOR in the presence or absence of GTPγS, although only RHEB-GTP was shown to activate mTORC1[4]. However, the binding affinity of RHEB- GTPγS to mTOR was five-fold weaker (K_D = 13.18 μM) than that of GTPγS-free RHEB (K_D = 2.44 μM; Figure 1e). This result suggests that a conformational change happens upon GTP binding to RHEB, leading to decrease of the binding affinity to mTOR. Because the GTP binding site is near the switch I of RHEB (33-41), the binding of GTP probably interferes the interaction between the switch I and mTOR domains involving M-heat and FAT [4].

The cryo-EM analysis revealed that RHEB interacted with three different mTOR fragments of 60-167 in N-heat domain (hereafter termed as ΔN), 967-1023 in M-heat domain (ΔM) and 1240-1360 in FAT domain (ΔFAT) (Figure 2a) [4]. On the other hand, RHEB is also reported to bind the fragment of 2148-2300 in the ATP binding domain (ΔATP), which is far from the RHEB binding site involving ΔN, ΔM and ΔFAT (Figure 2a) [10]. To reveal the binding properties of the mTOR fragments, we assayed the binding of RHEB to ΔN, ΔM, ΔN-M (ΔN + ΔM conjugates), ΔN-FAT-M (ΔN + ΔFAT + ΔM conjugates) and ΔATP by the split-luciferase technology (NanoBiT®; Promega, USA) (Figure S5) [16]. In the assay, the plasmids of RHEB-LgBiT and each mTOR fragment-SmBiT were co-transfected to HEK293 cells and incubated for 48 h. Then, the PPI was assayed by measuring the luminescence intensity initiated by the addition of luciferin (furimazine) (Figure 2b). For the analysis, we normalized the GTP concentration considering of the inherent GTP in cells. As a result, RHEB bound to all the mTOR fragments but with different affinities. The luminescence intensity of ΔN-M and ΔN-FAT-M fell into the same range, suggesting that ΔFAT was a little involved in the RHEB binding (Figure 2C). On the other hand, the single fragments of ΔN and ΔM showed a similar luminescence intensity, suggesting a same level of affinity (Figure 2c). In the bindings, the mTOR fragment conjugates of ΔN-M or ΔN-FAT-M showed higher affinity than those of ΔN and ΔM, which suggested the multiple-fragments could increase the binding affinity in a cooperation manner (Figure 2c). In addition, ΔATP showed the highest luminescence intensity, suggesting the strongest affinity for RHEB (Figure 2c). This result corresponds the previous report that RHEB bound ΔATP domain [10]. Since the ΔATP domain of mTOR (2148-2300) is highly conserved in the PI3K family [10,17], it is possible that RHEB regulates the kinase activity of mTOR upon the binding to ΔATP domain.

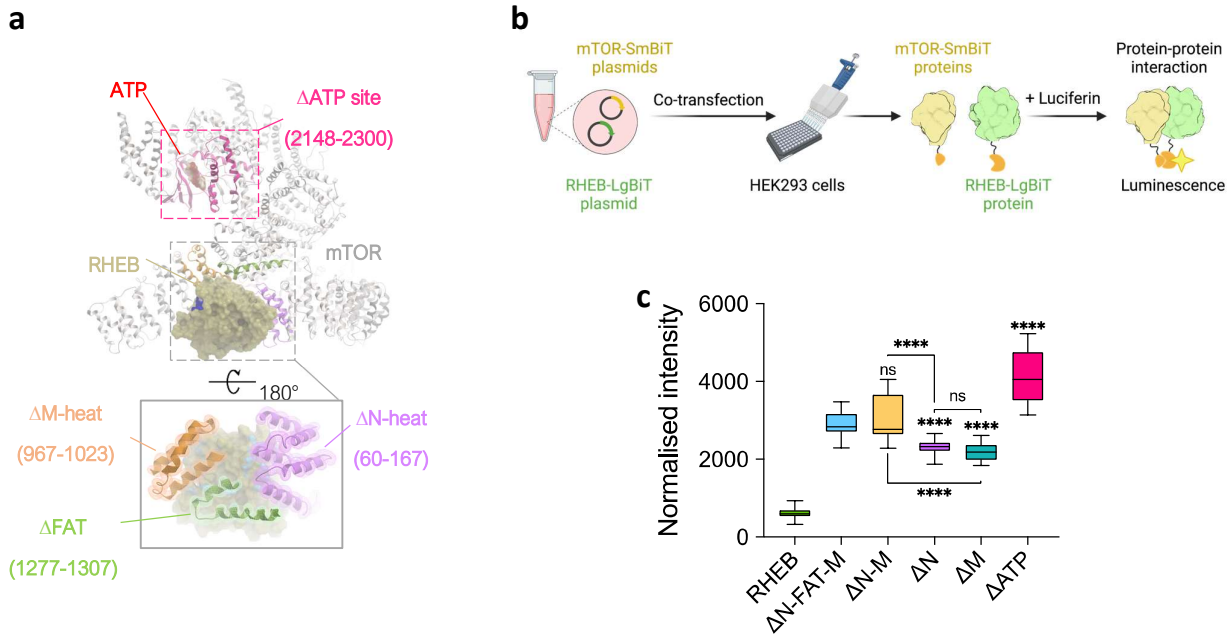

Figure 2. NanoBiT assay of RHEB binding to the different mTOR fragments. (**a**) The cryo-EM structure of RHEB complexed with mTOR (PDB ID: 6BCU) with indication of mTOR fragments. (**b** and **c**) In-cell NanoBiT assay to evaluate the binding of the RHEB-LgBiT with the SmBiT-plasmids of the different mTOR fragments. (**b**) The plasmids were co-transfected to HEK293 cells, incubated for 48 h, and the luminescence reaction was initiated by luciferin addition. (**c**) Luminescence of the mTOR fragments with RHEB. Data shown as mean ± standard deviation from a representative result of two independent experiments (n=6 replicates each). The signal was normalized to the background. Ordinary one-way ANOVA was used: ****$P < 0.0001$; ns, $P > 0.05$.

Preprints (www.preprints.org) | NOT PEER-REVIEWED | Posted: 11 June 2021 doi:10.20944/preprints202106.0309.v1

Based on the NanoBiT results, we further quantitatively measured the binding kinetics of RHEB with the mTOR fragments of ΔN-FAT-M, ΔN and ΔATP by the BLItz system (FortéBio, USA) [15]. For the measurements, we overexpressed the mTOR fragments by pET15b/BL21(DE3) E. coli system and purified them by Ni-NTA and Superdex-200 columns (GE Healthcare, USA) (Figure S6-S8). The 6xHis-tag was then cleaved by thrombin from RHEB and further purified by His SpinTrap column (GE Healthcare, USA) to remove the cleaved 6xHis-taggs, and then by benzamidine column (GE Healthcare, USA) to remove thrombin. After that, 1 μM 6xHis-tagged mTOR fragments of ΔN-FAT-M, ΔN or ΔATP were immobilized onto a Ni-NTA biosensor (FortéBio, USA) (Figure S9), and the 6xHis-tag cleaved-RHEB was used as analyte. As results, RHEB bound to the constructed allosteric binding site, ΔN-FAT-M, with K_D = 1.26 μM (Figure 3a-c, Table 1). On the other hand, ΔN showed a weaker affinity to RHEB with K_D = 6.47 μM (Figure 3d-f, Table 1), which corresponded to the in-cell results. Finally, RHEB bound to the ΔATP with the highest affinity of K_D = 29 nM (Figure 3g-i, Table 1), as suggested by the in-cell assay (Figure 2c). These different bindings obtained suggests the multiple functionalities of RHEB to regulate the kinase activity of mTORC1 [4]. We tried to measure the binding kinetics of the whole mTOR by the same method through the immobilization of RHEB onto the sensor and using mTOR as analyte, but we could not be due to the fast association/dissociation rates because of the large molecular weight of mTOR complexes.

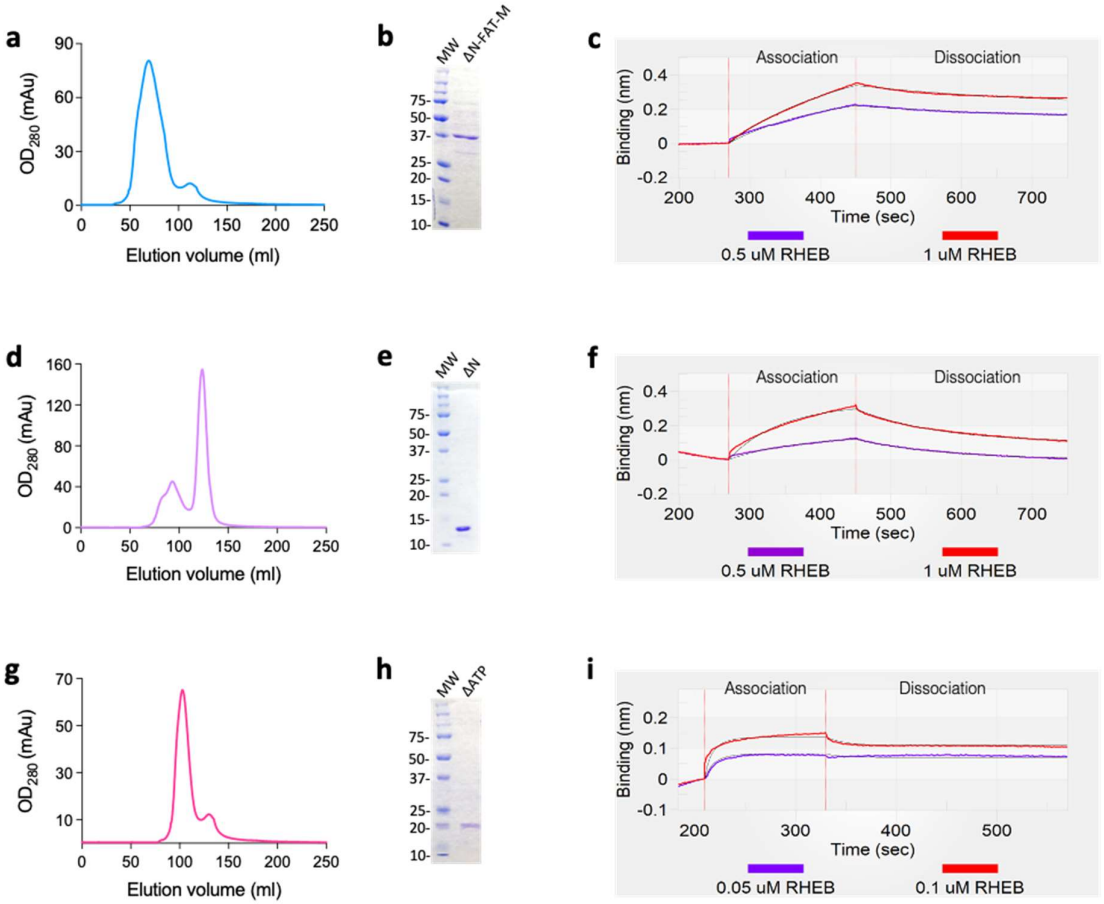

Figure 3. Binding kinetics of RHEB with mTOR fragments (1 μM) measured by BLItz. (**a** and **b**) Gel filtration profile (**a**) and the corresponding Coomassie-blue stained SDS-PAGE (**b**) of ΔN-FAT-M. (**c**) Binding of RHEB to ΔN-FAT-M with association and dissociation phases at 180 s and 300 s, respectively. (**d** and **e**) Gel filtration profile (**d**) and the corresponding Coomassie-blue stained SDS-PAGE (**e**) of ΔN. (**f**) Binding of RHEB to ΔN with association and dissociation phases at 180 s and 300 s, respectively. (**g** and **h**) Gel filtration profile (**g**) and the corresponding Coomassie-blue stained SDS-PAGE (**h**) of ΔATP. (**i**) Binding of RHEB to ΔATP with association and dissociation phases at 120 s and 240 s, respectively. Global fitting was carried out for 1:1 binding kinetics. The calculated parameters are shown in Table 1.

Preprints (www.preprints.org) | NOT PEER-REVIEWED | Posted: 11 June 2021 doi:10.20944/preprints202106.0309.v1

Table 1. Kinetic parameters of 1:1 binding model of RHEB with the indicated proteins.

Protein	K_D (M) [1*]	k_a (M^{-1} s^{-1}) [2*]	k_d (s^{-1}) [3*]	χ^2 [4]
ΔN-FAT-M	$1.26 \pm 0.11 \times 10^{-6}$	$2.00 \pm 0.12 \times 10^{3}$	$2.40 \pm 0.11 \times 10^{-3}$	0.04
ΔN	$6.47 \pm 0.13 \times 10^{-6}$	$1.51 \pm 0.30 \times 10^{3}$	$9.77 \pm 0.07 \times 10^{-3}$	0.04
ΔATP	$2.91 \pm 0.10 \times 10^{-8}$	$8.50 \pm 0.13 \times 10^{5}$	$2.47 \pm 0.03 \times 10^{-2}$	0.02

[1] K_D, equilibrium dissociation constant. [2] k_a, association rate constant. [3] k_d, dissociation rate constant. [4] χ^2, Chi-squared test of the fitted curve. * The values of K_D, k_a, and k_d are indicated ± the standard errors.

4. Materials and Methods

4.1. Materials

Reagent or resource	Source	Identifier
Antibodies		
Rabbit mAb anti-mTOR	Cell Signaling Technology	2983; RRID: AB_2105622
Goat anti-rabbit-HRP secondary antibody	Invitrogen, Thermo Fisher	A16104; RRID: AB_2534776
Bacterial Strains		
ECOS™ Competent *E. coli* DH5α	Nippon Gene	316-06233
ECOS™ Competent *E. coli* BL21(DE3)	Nippon Gene	312-06534
Chemicals and Recombinant Proteins		
Dpn1 enzyme	Takara	1235A
ExoSAP-IT enzyme	Bioscience, Thermo Fisher	75001.1
KOD one PCR enzyme mix	Toyobo	KMM-201
D-MEM (High-Glucose) media	FujiFilm Wako Pure Chemicals	044-29765
Opti-MEM media	Gibco, Thermo Fisher	31985-070
Fugene HD	Promega	E2311
Ampicillin, sodium salt	Nacalai Tesque	02739-32
Kanamycin	FujiFilm Wako Pure Chemicals	113-00343
Isopropyl β-D-1-thiogalactopyranoside (IPTG)	Nacalai Tesque	19742-94
Luria-Bertani agar media	Sigma-Aldrich	1002650948
Luria-Bertani Broth media	Nacalai Tesque	20068-75
Modified Terrific Broth media	Sigma-Aldrich	1002891164
Antifoam SI	FujiFilm Wako Pure Chemicals	018-17435
Protease inhibitors	Roche	06538282001
Thrombin	FujiFilm Wako Pure Chemicals	206-18411
GTPγS	Millipore	20-176
Commercial kits		
NucleoSpin® EasyPure kit	Macherey-Nagel	740727.50
NanoBiT® PPI Control Pair (FKBP/FRB)	Promega	N2016
Nano-Glo® Live Cell Assay System	Promega	N2012

Preprints (www.preprints.org) | NOT PEER-REVIEWED | Posted: 11 June 2021 doi:10.20944/preprints202106.0309.v1

Anti-Rabbit IgG Alpha Donor beads	PerkinElmer	AS105M
Anti-6xHis AlphaLISA Acceptor beads	PerkinElmer	AL178M
HaloTag protein purification system	Promega	G6270
In-Fusion cloning kit	Takara	639650
HisTrap™ HP Ni column	Cytiva	17524802
HisTrap™ FF crude Ni column	Cytiva	17528601
Superdex-200 HiLoad 16/60 column	GE Healthcare	28-9893-35
His SpinTrap™ column	GE Healthcare	28401353
HiTrap™ Benzamidine FF column	GE Healthcare	17-5143-02
PD spintrap G-25	GE Healthcare	28918004
Cell Lines		
HEK293	RIKEN Cell Bank	N/A
Oligonucleotides		
Synthetic human RHEB gene (507 bp) UniportKB ID: Q15382	Eurofins Genomics	GSY1601-1
Human mTOR ORF/pFN21A UniportKB ID: P42345	Kazusa Institute / Promega	FHC01207
pET15b vector	Novagen	69661
Primers for RHEB fragmentation for pET15b: FOR: GTGCCGCGCGGGCAGCCAGTCCAAAAGCCGCAAAATC REV: ATCGATAAGCTTCTATTCCAACT TTTCCGCTTCCAG	Eurofins Genomics	N/A
Primers for pET15b linearization: FOR: CATATGGCTGCCGCGCGGCACCAGGCCGCTGCTG REV: TAGAAGCTTATCGATGATAAGCTGTCAAACATGAG	Eurofins Genomics	N/A
Primers for RHEB fragmentation for LgBiT: FOR: ATCGCCATGGTGGCCCAGTCCAAAAGCCGCAAAATC REV: ACTGCCTTGAGAAACTTCCAACTTTTCCGCTTCC	Eurofins Genomics	N/A
Primers for LgBiT vector linearization: FOR: GTTTCTCAAGGCAGTTCAGGTGGTGGCGGGAGCGG REV: GGCCACCATGGCGATCGCTAGCGGTGGCTTTACC	Eurofins Genomics	N/A
Primers for SmBiT vector linearization: FOR: TGGGCTAGCAGATCTTCTAGAGTCGGGGCGGCCGG REV: CATTCCACCGCTCGAGCCTCCACCTCCGCTCCCGC	Eurofins Genomics	N/A
Primers for mTOR$^{\Delta N}$ Fragment for SmBiT: FOR: GGCTCGAGCGGTGGATCTACTCGCTTCTATGACC REV: AGAAGATCTGCTAGCACCCAGCCATTCCAGGGC	Eurofins Genomics	N/A
Primers for mTOR$^{\Delta M}$ Fragment for SmBiT: FOR: GGCTCGAGCGGTGGACATCACACCATGGTTGTCC REV: AGAAGATCTGCTAGCCACAAAGGACACCAACATTC	Eurofins Genomics	N/A
Primers for mTOR$^{\Delta N\text{-}M}$ Fragment for SmBiT: FOR: ACATGCACATCACACCATGGTTGTCCAGGCCATC REV: GTGTGATGTGCATGTCTCCGGCCCTCATTGCGG	Eurofins Genomics	N/A
Primers for mTOR$^{\Delta N\text{-}F\text{-}M}$ Fragment for SmBiT: FOR: GGCCGGAGACATGCAGGCCAAGGGGATGCATTGG REV: AACCATGGTGTGATGCAAGTTTAAGAGGGTCTGTG	Eurofins Genomics	N/A
Primers for mTOR$^{\Delta Ki}$ Fragment for SmBiT: FOR: GCTCGAGCGGTGGACAGCCAATCATTCGCATTCAG REV: AGAAGATCTGCTAGCGGCCAGGTCGTCCCCAGCTG	Eurofins Genomics	N/A
Primers for mTOR$^{\Delta N}$ Fragment for pET15b: FOR: GTGCCGCGCGGCAGCTCTACTCGCTTCTATGACC REV: ATCGATAAGCTTCTAACCCAGCCATTCCAGGGCTC	Eurofins Genomics	N/A

 doi:10.20944/preprints202106.0309.v1

Primers for mTOR$^{\Delta N\text{-}F\text{-}M}$ Fragment for pET15b: FOR: GATAACGCGATCGCCTCTACTCGCTTCTATGACC REV: CGAATTCGTTTAAACCACAAAGGACACCAACATTC	Eurofins Genomics	N/A
Primers for mTOR$^{\Delta Ki}$ Fragment for pET15b: FOR: GATAACGCGATCGCCCTGCCTCAGCTCACATCC REV: CGAATTCGTTTAAACGCATGTGATTCTGTAGTTGC	Eurofins Genomics	N/A
Primers for colony PCR of SmBiT/LgBiT: FOR: GAAGTCGAACACGCAGATGCAGTCG REV: CACTGCATTCTAGTTGTGGTTTGTCCAAACTC	Eurofins Genomics	N/A
Primers for colony PCR of pET15b: FOR: CGATCCCGCGAAATTAATACGACTCACTATAG REV: GACATTAACCTATAAAAATAGGCGTATCACGAGG	Eurofins Genomics	N/A
Software		
ICM-Pro 3.9 software	Molsoft L.L.C.	https://www.molsoft.com/products.html
SnapGene 5.1.7 software	GSL Biotech L.L.C.	https://www.snapgene.com/
BLItzPro 1.2 software	FortéBio (Sartorius)	https://www.sartorius.com/
Prism 8.4.3 software	GraphPad	https://www.graphpad.com/

4.2. Methods

4.2.1. mTOR expression and purification

Human mTOR ORF was supplied in pFN21A HaloTag® CMV Flexi® Vector which was handled as previously described1, 2. Briefly, HEK293 cells were transfected by the Halo-tagged mTOR using FuGene HD transfection agent and grown as monolayer in 10-cm plates. Then, the cells (108) were collected and lysed on ice by 50 mM HEPES, pH 7.5, 150 mM NaCl, 1 mM EDTA, 1%(v/v) Triton X-100, 10 %(v/v) glycerol, 0.1%(w/v) sodium deoxycholate, 0.005%(v/v) IGEPAL buffer containing protease inhibitors and 1.6 µg/ml DNase I. Cell lysate was then, centrifuged at 13,200g for 30 min at 4°C and the pellet was discarded. The supernatant was incubated with the pre-equilibrated HaloLink resin for 1 h at room temperature on rotor. Then, the resin was washed three times by the purification buffer. After that, mTOR was released from the resin by the TEV protease cleavage for further 1 h at room temperature on rotor. The released mTOR in the supernatant was carefully removed and incubated with Ni-NTA resin to remove the 6xHis-proteolytic TEV. Finally, the last supernatant containing mTOR was replaced by storage buffer (50 mM HEPES, pH 7.5, 10 %(v/v) glycerol) and concentrated to be stored at -80 °C. The yield was examined by western blotting using anti-mTOR antibody.

4.2.2. Western blotting

Western blotting was performed as previously described 3 to check mTOR expression and purification steps. After SDS-PAGE, the protein bands were transferred onto PVDF membrane (Millipore) using Trans-Blot Transfer System (Bio-Rad). Then, the membrane was blocked for 1 h at room temperature with 4% w/v skimmed milk 1× TBS-T, and after wash, it was incubated for 1 h at room temperature with primary antibody against mTOR followed by the goat anti-rabbit secondary antibody incubation at room temperature or 2 h. Finally, the membranes images were collected using the WSE-6100 LuminoGraph I (ATTO).

4.2.3. Preparation of RHEB and mTOR truncates

a. Plasmid construction

The proteins were prepared by the pET15b expression vector and BL21(DE3) E. coli.4, 5 Briefly, RHEB (507 bp), ΔN-FAT-M (858 bp), ΔN (294 bp), and ΔATP (459 bp) genes were cloned into pET15b expression vector using In-fusion cloning kit. The constructed plasmids were transformed into DH5α E. coli and spread over LB agar plates containing 0.1 mM ampicillin. Colony PCR and gene sequencing were performed to confirm the genes constructions, and the plasmids were purified using NucleoSpin® Plasmid EasyPure kit according to the manufacturer protocol. Then, the purified plasmids were transformed into BL21(DE3) E. coli and incubated at 37°C for 6h in LB media containing 0.1 mM

ampicillin. The proteins expressions were induced by 1 mM IPTG and further incubated overnight at 37°C. SDS-PAGE showed that RHEB and ΔN were expressed as a soluble protein while ΔN-FAT-M and ΔATP were expressed as inclusion body.

b. Protein expression

At day 1, 5 L Terrific broth media, TB were prepared containing 0.8% (v/v) glycerol and autoclaved. Parallelly, a 5 ml starter cultures were prepared as described above without IPTG and incubated overnight at 37°C. At day 2, 0.1 mM ampicillin and 1% (v/v) antifoam SI solution were added to the TB media and OD600 was checked as a reference. The starter cultures were added to the TB flasks and incubated at 37 °C with shaking (110 rpm). The OD600 values were measured hourly till reached ≥ 1.0, then 1mM IPTG was added and further incubated for overnight was followed. At day 3, cultures solutions were centrifuged at 8000 rpm (15 min, 4 °C), and cell pastes were stored at -80°C.

c. Protein purification

Cell pasts (5 g for insoluble proteins or 10 g for soluble proteins) were resuspended in 100 ml lysis buffer (50 mM Tris-HCl, pH 8.0, 100 mM NaCl, 1mM EDTA, 0.04 mg/ml lysozyme, 0.16 mg/ml DNase I) supplemented with 1x protease inhibitor and the suspension was disrupted using cell disruptor (5.0 W, 30-40 % cycle / sec, 5 min) on ice. For soluble proteins, cell lysate was ultra-centrifuged at 40,000 rpm for 1h at 4 °C and the pellet was discarded. Then, the supernatant was applied to the HisTrapTM HP Ni-NTA column powered by AKTAprime plus FPLC (GE Healthcare) using binding buffer (50 mM Tris-HCl, pH 8.0, 10 % v/v glycerol) and eluted by a gradient (0-100%) elusion buffer (50 mM Tris-HCl, 10 % v/v glycerol, 1M imidazole, pH 8.0). The peak fractions were checked by SDS-PAGE, pooled, and loaded onto 3 KDa molecular weight cut-off Amikon® filter (Millipore) for washing by the binding buffer. Finally, proteins were concentrated and stored at -80 °C.

The recombinant ΔN-FAT-M and ΔATP had been expressed as inclusion bodies so, the purification process involved a refolding step. After cell disruption, the lysate was centrifuged at 8000 rpm for 5 min at 4 °C. Then, the pellet was washed 3 times by washing buffer (50 mM Tris-HCl, 100 mM NaCl, 1 mM EDTA, 4 M urea, pH 8.0) followed by other 3 times washing by the same buffer without urea. The pellet was then resuspended in 20 ml solubilization buffer (50 mM Tris-HCl, 8 M urea, 100 mM NaH2PO4, 10 mM 2-mercatoethanol, pH 8.0) on rotor for 2 h at room temperature. After centrifugation (40,000 rpm, 1 h, 4°C), the supernatant was diluted by the binding buffer (50 mM Tris-HCl, 8 M urea, 100 mM NaH2PO4, 5 mM 2-mercatoethanol, pH 8.0) and loaded onto HisTrapTM FF crude Ni-NTA column (GE Healthcare). After binding, the protein was eluted by a gradient (0-100%) elusion buffer (50 mM Tris-HCl, 8 M urea, 100 mM NaH2PO4, 5 mM 2-mercatoethanol, 1 M imidazole, pH 8.0). The peak fractions were checked by SDS-PAGE, pooled, and dropped into refolding buffer (50 mM Tris-HCl, 40 mM NaCl, 1 mM EDTA, 1 M L-arginine and 10 % v/v glycerol, pH 8.0). The refolded sample was then washed over 3KDa MW-CO filter by the gel filtration buffer. After that, proteins were subjected for gel filtration using Superdex-200 column using running buffer of 50 mM Tris-HCl, pH 8.0, 150 mM NaCl, 10 % v/v glycerol. After SDS-PAGE purity confirmation, the purified fractions were collected, concentrated, and stored at -80 °C.

4.2.4. His-tag cleavage from RHEB

A ratio of 1 mg protein in 20 times 1X PBS: 10 units of thrombin was prepared and incubated for 16 h at room temperature on rotor to cleave the 6-His tag at the thrombin site. Then, the solution was passed over the His SpinTrapTM column to remove 6-His tag which eluted by 100-, 200- and 500-mM imidazole in 1X PBS, respectively. Following the fractionation and to remove thrombin, the solution was loaded onto HiTrapTM Benzamidine FF column by the binding buffer C (50 mM Tris-HCl, 100 mM NaCl, pH 8.0) to be gradually (0-100 %) eluted by the elution buffer B (50 mM Tris-HCl, 500 mM NaCl, pH 8.0).

4.2.5. RHEB charging with GTPɣS

We followed the RHEB charging protocol as previously described with some modifications6. RHEB was incubated with 20-fold molar excess of GTPɣS in the presence of 10 mM EDTA for 20 min at room temperature. Finally, the reaction was stopped by the addition of 20 mM of MgCl2. The yield was then passed over PD spintrap G-25 column to remove excess GTPɣS.

 doi:10.20944/preprints202106.0309.v1

4.2.6. AlphaLISA assay for RHEB-mTOR protein: protein interaction

A protein: protein interaction (PPI) assay based on energy transfer via donor/acceptor system using AlphaLISA® assay (PerkinElmer) was used7. Briefly, 100 μg/ml anti-IgG donor beads was incubated with excess anti-mTOR antibody for 1 h at room temperature followed by washing by 1x dilution buffer supplemented with the beads to remove unbound anti-mTOR antibodies. Then, final concentration of 10 nM of purified mTOR was added to the donor beads solution and further incubated for 1 h at room temperature. After beads washes, the donor beads-mTOR complex was aliquoted (4 μl) in a 384-well OptiPlateTM (PerkinElmer). Then, 6xHis-RHEB or 6xHis-RHEB-GTPɣS was titrated (3 μl of 0.1-100 μM) into the donor beads-mTOR mix and shaken gently. Finally, 3 μl of 200 μg/ml anti-6His acceptor beads were added to the mixture, the plate was top-sealed, covered and incubated for more than 1h at room temperature in dark. The alpha signals were then measured by EnSpireTM plate reader (PerkinElmer).

4.2.7. Preparation of plasmids of in-cell protein: protein interaction (NanoBiT assay)

RHEB (507 bp) gene was cloned into LgBiT vector, and ΔN-FAT-M (858 bp), ΔN-M (495 bp), ΔN (294 bp), ΔM (171 bp) and ΔATP (459 bp) genes were cloned into SmBiT vector using In-fusion cloning kit. The constructed plasmids were transformed into Dh5α e. coli and spread over LB agar plates containing 0.1 mM ampicillin. Colony PCR and gene sequencing were performed to confirm the genes constructions, and the plasmids were purified using NucleoSpin® Plasmid EasyPure kit according to the manufacturer protocol.

4.2.8. In-cell NanoBiT assay

The NanoLuc Binary Technology (NanoBiT) based on split Luciferase subunits can be used for the intracellular detection of PPI8. Briefly, 104 HEK293 cells were seeded in D-MEM (10% FBS; 1% P/S) in B&W Isoplate-96 TC (PerkinElmer) and incubated overnight (5% CO2; 37°C). Then, the RHEB-LgBiT vector with the different SmBiT variants (50 ng/well each) were co-transfected into the cells using FuGENE HD at a ratio of 3:1 (v/w) and incubated for 48 h (5% CO2; 37ºC) for protein expression. Then, the culture medium was replaced by Opti-MEM reduced serum medium, and 20 μl of 20× diluted furimazine was injected for luciferase interaction initiation; the luminescence signal was measured using EnSpire plate reader (PerkinElmer).

4.2.9. BLItz measurements of RHEB interactions with mTOR truncates

We used the BLItz instrument (FortéBio, USA) to measure the binding kinetics of RHEB with the truncated mTOR fragment. At first, Ni-NTA biosensors (FortéBio, USA) was hydrated for 2 h in the kinetics buffer (10 mM HEPES, pH 7.4, 100 mM NaCl, 0.02% v/v Tween-20 and 5 mg/ml bovine serum albumin). In all measurements the his-tagged truncated mTOR fragments (1 μM) were used as ligands to be immobilized onto the sensors, while tagless RHEB was used as analyte. In case of ΔN-FAT-M or ΔN, the measurement cycle composed of 30s initial baseline (buffer), 120s ligand loading, 120s baseline (buffer), 180s analyte association and 300s dissociation phases (buffer) while for ΔATP, the cycle was shorter and divided into 30s, 120s, 60s, 120s and 240s, respectively. A reference cycle was applied for each sensor by introducing analyte only in the association phase to exclude nonspecific binding possibilities. RHEB concentrations were 0.5 and 1 μM ΔN-FAT-M or ΔN, and 0.05 and 0.1 μM for ΔATP. Finally, the binding curves were fitted using 1:1 binding kinetics and analyzed by the BLItzPro 1.2 software (FortéBio, USA).

4.2.10. Data analysis

Statistical significance and number of samples are noted in the figure legends where appropriate. Data are expressed as mean ± SD. Ordinary one-way ANOVA was used as indicated; **** for $P < 0.0001$, *** for $P < 0.001$, ** for $P < 0.01$, * for $P < 0.05$, and ns for $P > 0.05$. Statistical analyses were performed using GraphPad Prism software, v.8.4.3.

5. Conclusion

Although the previous studies showed that RHEB-GTP activated mTORC1 by several mechanisms, they did not reveal the binding kinetics [4,8,10]. Here we studied the binding details of RHEB to whole mTOR and the truncated mTOR fragments [4,10]. In the assays, we used the in-cell and in vitro assays to facilitate the measurements [18]. RHEB

bound to whole mTOR with 5 times weaker affinity in the presence of GTP than that of GTP absence. On the other hand, the binding study of the truncated mTOR fragments involved in the allosteric binding site suggested the cooperative binding mode for RHEB. In addition, we observed that RHEB bound to the truncated ATP binding site in-cell and in vitro. The results show that the binding of RHEB to mTOR involves multiple binding sites with a variety of biding affinities, suggesting that RHEB regulates the kinase activity of mTOR through multiple mechanism.

Supplementary Materials: Supplementary note 1: Human mTOR gene sequence; Supplementary note 2: Human RHEB gene sequence; Figure S1: On-lysosome activation of mTORC1 by RHEB; Figure S2: Construction and purification of overexpressed mTOR; Figure S3: Construction and purification of overexpressed RHEB; Figure S4: The established AlphaLISA method for RHEB-mTOR interaction; Figure S5: The constructed plasmids for NanoBiT assay. Figure S6: Construction and purification of overexpressed ΔN-FAT-M; Figure S7: Construction and purification of overexpressed ΔN; Figure S8: Construction and purification of overexpressed ΔATP; Figure S9: Schematic illustration showing BLItz measurement steps.

Author Contributions: H.M. and R.S. conceived the whole project. Y.I. managed the research group. R.S. designed and conducted the experimental works. R.S. and H.M. wrote the manuscript. All authors checked and approved the experimental results and the manuscript.

Funding: R.S. was supported by the Junior Research Associate (JRA) Program in RIKEN. H.M. was partly supported by the Incentive Research Program in RIKEN (FY2018-2019, FY2019-2020) and JSPS Grant-in-Aid for Scientific Research (C) (JP20K06516).

Acknowledgment: We are grateful to the Support Unit for Bio-material Analysis, RIKEN CBS Research Resources Center (RRC) for DNA sequencing. We thank Editage (https://www.editage.jp/) for the English language revision.

Conflict of Interest: The authors declare no competing interests.

Abbreviations:

ATP	Adenine triphosphate
4EB-P1	Eukaryotic translation initiation factor 4E-binding protein 1
Da	Dalton
FKBP12	FK506 binding protein of 12-KDa
GTPγS	Non-hydrolysable guanidine triphosphate
LgBiT	Large fragment of the NanoLuc Binary Technology (NanoBiT)
mTOR	Mammalian/Mechanistic target of rapamycin
PI3K	Phosphoinositide 3-kinases
PPI	Protein: protein interaction
SmBiT	Small fragment of the NanoLuc Binary Technology (NanoBiT)
RHEB	Ras homolog enriched in brain protein
S6K1	Ribosomal protein S6 kinase 1
TSC	Tuberous sclerosis complex
RAPTOR	Regulatory-associated protein of mTOR
DEPTOR	DEP domain containing protein 6
mLST8	Mammalian lethal with SEC13 protein 8
PRAS40	40 KDa proline-rich AKT substrate

References

1. Liu, G.Y.; Sabatini, D.M. mTOR at the Nexus of Nutrition, Growth, Ageing and Disease. Nat Rev Mol Cell Biol 2020, 21, 183-203, doi:10.1038/s41580-019-0199-y.

2. Mossmann, D.; Park, S.; Hall, M.N. mTOR Signalling and Cellular Metabolism are Mutual Determinants in Cancer. *Nat Rev Cancer* **2018**, *18*, 744-757, doi:10.1038/s41568-018-0074-8.

3. Saxton, R.A.; Sabatini, D.M. mTOR Signaling in Growth, Metabolism, and Disease. *Cell* **2017**, *169*, 361-371, doi:10.1016/j.cell.2017.03.035.

4. Yang, H.; Jiang, X.; Li, B.; Yang, H.J.; Miller, M.; Yang, A.; Dhar, A.; Pavletich, N.P. Mechanisms of mTORC1 Activation by RHEB and Inhibition by PRAS40. *Nature* **2017**, *552*, 368-373, doi:10.1038/nature25023.
5. Shen, K.; Sabatini, D.M. Ragulator and SLC38A9 activate the Rag GTPases through noncanonical GEF mechanisms. *Proc Natl Acad Sci U S A* **2018**, *115*, 9545-9550, doi:10.1073/pnas.1811727115.
6. Saxton, R.A.; Chantranupong, L.; Knockenhauer, K.E.; Schwartz, T.U.; Sabatini, D.M. Mechanism of arginine sensing by CASTOR1 upstream of mTORC1. *Nature* **2016**, *536*, 229-233, doi:10.1038/nature19079.
7. Heard, J.J.; Fong, V.; Bathaie, S.Z.; Tamanoi, F. Recent progress in the study of the Rheb family GTPases. *Cell Signal* **2014**, *26*, 1950-1957, doi:10.1016/j.cellsig.2014.05.011.
8. Bai, X.; Ma, D.; Liu, A.; Shen, X.; Wang, Q.J.; Liu, Y.; Jiang, Y. RHEB Activates mTOR by Antagonizing its Endogenous Inhibitor, FKBP38. *Science* **2007**, *318*, 977-980, doi:10.1126/science.1147379.
9. Long, X.; Ortiz-Vega, S.; Lin, Y.; Avruch, J. Rheb binding to mammalian target of rapamycin (mTOR) is regulated by amino acid sufficiency. *J Biol Chem* **2005**, *280*, 23433-23436, doi:10.1074/jbc.C500169200.
10. Long, X.; Lin, Y.; Ortiz-Vega, S.; Yonezawa, K.; Avruch, J. Rheb binds and regulates the mTOR kinase. *Curr Biol* **2005**, *15*, 702-713, doi:10.1016/j.cub.2005.02.053.
11. Mahoney, S.J.; Narayan, S.; Molz, L.; Berstler, L.A.; Kang, S.A.; Vlasuk, G.P.; Saiah, E. A Small Molecule Inhibitor of Rheb Selectively Targets mTORC1 Signaling. *Nat Commun* **2018**, *9*, 548, doi:10.1038/s41467-018-03035-z.
12. Castro, A.F.; Rebhun, J.F.; Clark, G.J.; Quilliam, L.A. RHEB Binds Tuberous Sclerosis Complex 2 (TSC2) and Promotes S6 Kinase Activation in a Rapamycin- and Farnesylation-Dependent Manner. *J Biol Chem* **2003**, *278*, 32493-32496, doi:10.1074/jbc.C300226200.
13. Rogala, K.B.; Gu, X.; Kedir, J.F.; Abu-Remaileh, M.; Bianchi, L.F.; Bottino, A.M.S.; Dueholm, R.; Niehaus, A.; Overwijn, D.; Fils, A.P., et al. Structural basis for the docking of mTORC1 on the lysosomal surface. *Science* **2019**, *366*, 468-475, doi:10.1126/science.aay0166.
14. Anandapadamanaban, M.; Masson, G.R.; Perisic, O.; Berndt, A.; Kaufman, J.; Johnson, C.M.; Santhanam, B.; Rogala, K.B.; Sabatini, D.M.; Williams, R.L. Architecture of Human Rag GTPase Heterodimers and their Complex with mTORC1. *Science* **2019**, *366*, 203-210, doi:10.1126/science.aax3939.
15. Ning, B.; Ren, X.; Hagiwara, K.; Takeoka, S.; Ito, Y.; Miyatake, H. Development of a Non-IgG PD-1/PD-L1 Inhibitor by in Silico Mutagenesis and an In-Cell Protein-Protein Interaction Assay. *ACS Chem Biol* **2021**, *16*, 316-323, doi:10.1021/acschembio.0c00817.
16. Dixon, A.S.; Schwinn, M.K.; Hall, M.P.; Zimmerman, K.; Otto, P.; Lubben, T.H.; Butler, B.L.; Binkowski, B.F.; Machleidt, T.; Kirkland, T.A., et al. NanoLuc Complementation Reporter Optimized for Accurate Measurement of Protein Interactions in Cells. *ACS Chem Biol* **2016**, *11*, 400-408, doi:10.1021/acschembio.5b00753.
17. Gehrmann, T.; Heilmeyer, L.M., Jr. Phosphatidylinositol 4-kinases. *Eur J Biochem* **1998**, *253*, 357-370, doi:10.1046/j.1432-1327.1998.2530357.x.
18. Ning, B.; Ren, X.; Hagiwara, K.; Takeoka, S.; Ito, Y.; Miyatake, H. Development of a Non-IgG PD-1/PD-L1 Inhibitor by in Silico Mutagenesis and an In-Cell Protein-Protein Interaction Assay. *Acs Chem Biol* **2021**, 10.1021/acschembio.0c00817, doi:10.1021/acschembio.0c00817.